An Octave Band Switched Parasitic Beam-Steering Array

Adrian Sutinjo, *Student Member, IEEE*, Michal Okoniewski, *Senior Member, IEEE*, and Ronald H. Johnston, *Life Senior Member, IEEE*

***Abstract*—In this letter, we introduce a new parasitic antenna array with a 360° switchable coverage in the azimuthal plane. Unlike most switched parasitic arrays which are narrowband or at most dual band, this array covers an octave bandwidth. The frequency band of interest in this letter is the UHF band, particularly the 225–450 MHz tactical communication band. The array consists of a driven element surrounded by two layers of parasitic elements. The driven element is a wire frame biconical antenna and the parasitic elements are V-shaped bent wires. The proof-of-concept was simulated using FEKO method of moments (MoM) package and further verified using Ansoft HFSS. Simulation results show that the antenna gain is 6–10 dBi over an octave bandwidth.**

***Index Terms*—Beam-steering, circular array, ESPAR antenna, parasitic array, wideband antenna.**

I. Introduction

THE theoretical concept of beam-forming using a circular parasitic array was initially introduced by Harrington in 1978 [1]. The idea is to control the array radiation pattern by optimizing the values of reactive elements at the ports of the parasitic components which surround a single driven element. In such a configuration, beam-steering can be achieved by exciting only one element. In contrast, for a phased array antenna, *every* antenna element in the array is typically excited. Harrington's parasitic array is therefore simpler and less expensive to manufacture.

In recent years, there has been a resurgence of interest in Harrington's idea. Parasitic antenna array prototypes have been developed by other researchers and implemented with various beam-forming algorithms. An extensive review of modern work in this field can be seen in [2]. Lately, the parasitic beam-forming array is more widely known as the electronically steerable passive array radiator antenna (ESPAR) [2]. These terms will be used interchangeably in this letter to refer to Harrington's idea and/or its modern counterparts.

Further simplification to the ESPAR was proposed recently [3]. Instead of using dc-tuned reactive elements such as varactor diodes, the reactive loading is achieved by selective switching from among a few discrete reactive components. In this manner, the number of possible beams are limited by the allowable values. The advantage of this approach is that the beam-forming algorithm becomes simpler. An exhaustive search from among the allowed combination of reactive components can be performed to achieve the best signal-to-interference-and-noise-ratio (SINR) [3]. Most importantly, this approach eliminates the difficulties associated with the varactor diodes' voltage breakdown and nonlinearity. These issues are especially severe since the transmitter RF power level of a UHF tactical radio is high (up to 100 W). When passive components are used as loading components, the power handling issue is largely removed.

While much research has been done on the ESPAR, relatively little work has focused on overcoming the inherent narrow bandwidth associated with it. Most ESPARs consist of resonant linear dipole or monopole elements which are narrowband. Furthermore, the mutual coupling between the elements, by which the beam-forming is achieved, is a function of frequency. There have been some efforts in extending the varactor tunable ESPAR to dual-band operation [4]. Also, dual-band switched parasitic ESPARs have been demonstrated [5], [6]. In all of the aforementioned research, however, the two bands are well separated in frequency (typically, $f_{\text{high}} \sim 2 \cdot f_{\text{low}}$) and each band remains narrow ($\sim$10–15%). When it comes to broadband ESPAR, the array with the widest frequency range of operation was demonstrated in [7]; this array covers the 1.5–2.1 GHz band ($f_{\text{high}}/f_{\text{low}} = 1.4 : 1$) with the measured gain between 5–6 dBi.

In this letter, we present the design of a switched parasitic ESPAR covering the 225–450 MHz frequency band ($f_{\text{high}}/f_{\text{low}} = 2 : 1$) with simulated gain of 6–10 dBi in the entire range. The array structure and the beam-forming mechanism are explained in Section II. Section III discusses the simulated antenna performance as predicted by FEKO MoM and Ansoft HFSS simulation packages. Concluding remarks are made in Section IV.

II. The Parasitic Array Structure

The array is composed of the driven element and two layers of parasitics, as shown in the cross section sketch in Fig. 1. The driven element is a wireframe biconical antenna which, if placed in free space, would cover the 225–450 MHz band. The inner layer of parasitics are used for high band beam-forming, while the outer ones primarily affect the low band radiation. The wireframe biconical and each layer of the parasitics consist of 12 wire elements placed at 30° angular spacing between adjacent elements. A 3-D drawing of the array is shown in Fig. 2.

Beam-forming is achieved by judiciously switching the correct loading at the vertices of the parasitic elements. Three possible loads have been chosen for each element: open, short, and inductor. For the inner layer, the inductor value (L_{in}) was chosen to be 100 nH, while the outer inductor (L_{out}) values are

Manuscript received November 3, 2006; revised March 1, 2007. This work was supported by General Dynamics Canada, Calgary, AB, Canada, and by the Canadian Natural Sciences and Engineering Research Council.

The authors are with the Department of Electrical and Computer Engineering, the University of Calgary, Calgary, AB T2N 1N4, Canada (e-mail: okoniews@ucalgary.ca).

Digital Object Identifier 10.1109/LAWP.2007.895284

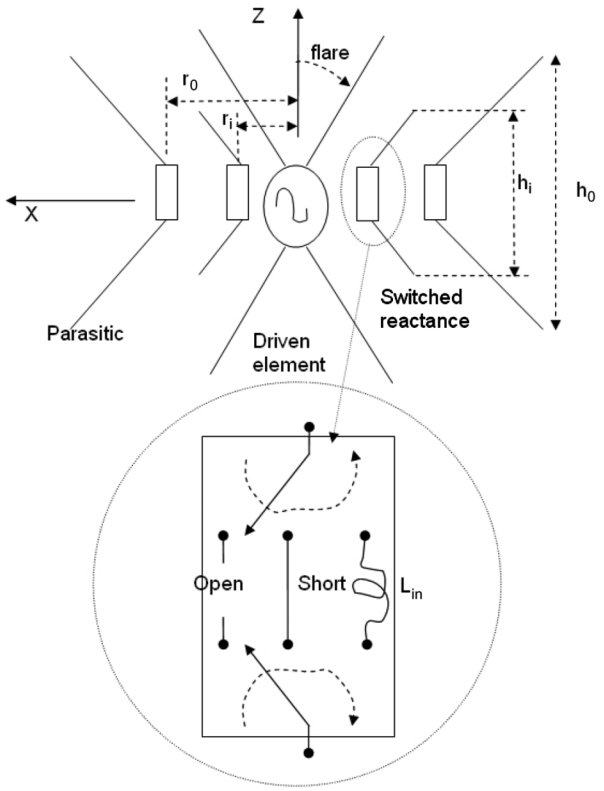

Fig. 1. Cross-section view of the octave band switched parasitic beam-steering array.

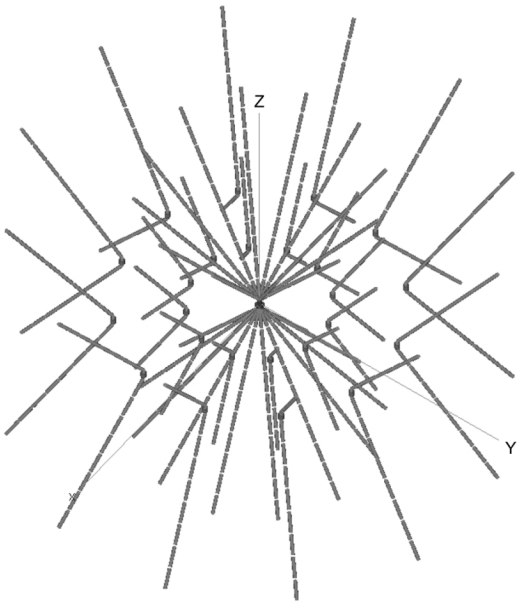

Fig. 2. 3-D view of the array.

68 nH. These values have been selected such that the electrical length for each parasitic element is appropriate for the high or low band beam-forming mode, which will be discussed in the following.

The entire 225–450 MHz band is covered with two partially overlapping beam-steering modes: low and high band. Fig. 3 illustrates cross section view of the array in the low and high band modes. To form a directive beam at the low band, all the inner parasitic elements and six adjacent outer parasitic elements are open circuited, while the remaining six outer parasitic elements are connected to L_{out}. In this manner all of the open circuited parasitic elements are nearly invisible while the ones connected to L_{out} behave as reflectors. Similarly, for the high band, all of the outer parasitic elements are open circuited. Six adjacent inner parasitic elements are connected to L_{in}, while the remaining six are short circuited. In this case, the shorted inner parasitic elements along with the open circuited outer parasitic elements directly in front of them behave as directors. The inner parasitic elements connected to the L_{in} act reflectors and effectively shadow the outer elements behind them.

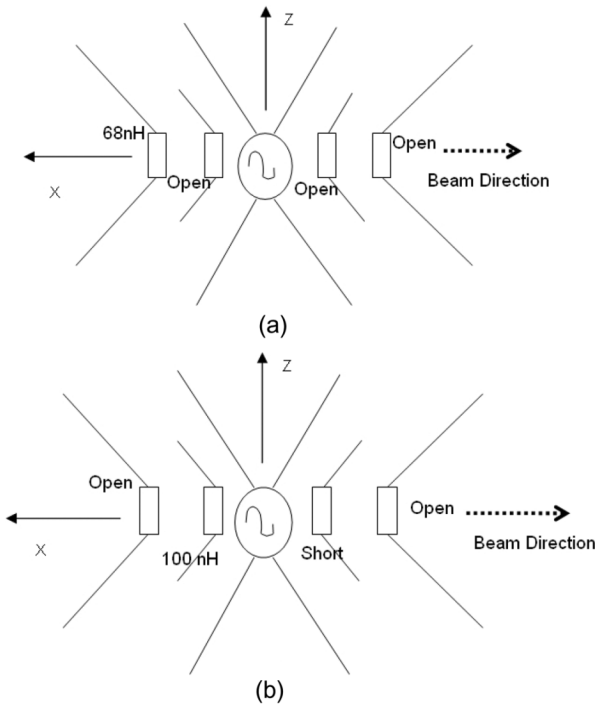

Fig. 3. Beam-forming at the (a) low- and (b) high-band modes.

The one octave gain bandwidth performance is achieved due to two main factors. First, the low- and high-band modes have been designed such that their gain bandwidths partially overlap in the middle of the 225–450 MHz band. The combination of the two modes allows coverage of the entire band. Second, the biconical driven element provides a more desirable antenna input impedance over the desired frequency band. In contrast to the resonant dipole or monopole which are used for the center element in a typical ESPAR, the wireframe bicone does not exhibit sharp anti resonances at the even harmonics of the lowest resonance frequency. These characteristics and the simulated performance of the antenna are further illustrated in the following section.

III. Simulation Results

The array with the dimensions shown in Table I with wire radius of 2.93 mm was simulated in the FEKO MoM package. The MoM is a well understood and accepted method for simulating wire antennas. Ansoft HFSS, which is a finite-element method (FEM) package, was used to verify FEKO on some key results. In HFSS, flat thin metal pieces which are 1 cm in width were used instead of the cylindrical wires for improved numerical efficiency.

TABLE I
ARRAY PARAMETERS

Driven Element	
h_c	$flare$
0.418λ	$35°$

Outer Layer		
h_o	r_o	L_{out}
0.3575λ	0.165λ	68 nH

Inner Layer		
h_i	r_i	L_{in}
$0.5 \cdot h_o$	$0.5 \cdot r_o$	100 nH

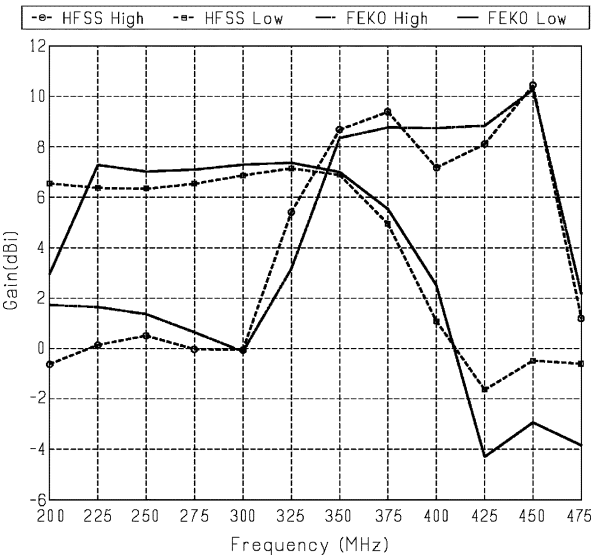

Fig. 4. Main beam ($\phi = 180°, \theta = 90°$) gain ($\hat{\theta}$ polarized) versus frequency.

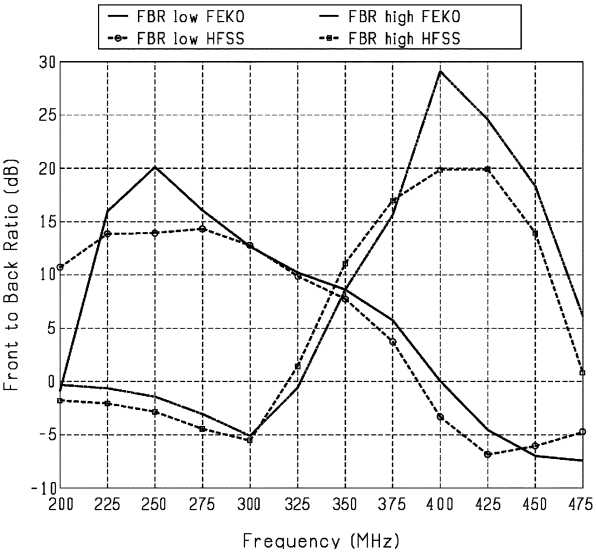

Fig. 5. Front-to-back ratio versus frequency.

Fig. 4 illustrates the gain of the array in the main beam direction versus frequency. The low band has a passband from roughly 225–350 MHz with a gain of greater than 6 dBi, whereas the high band has a passband from 350–450 MHz with at least 7 dBi of gain. Both HFSS and FEKO predict similar passband and stopband behavior. Further, Fig. 5 depicts the front-to-back (FBR) ratio of the array. It can be seen that the FBR is, for the most part, better than 10 dB except around the

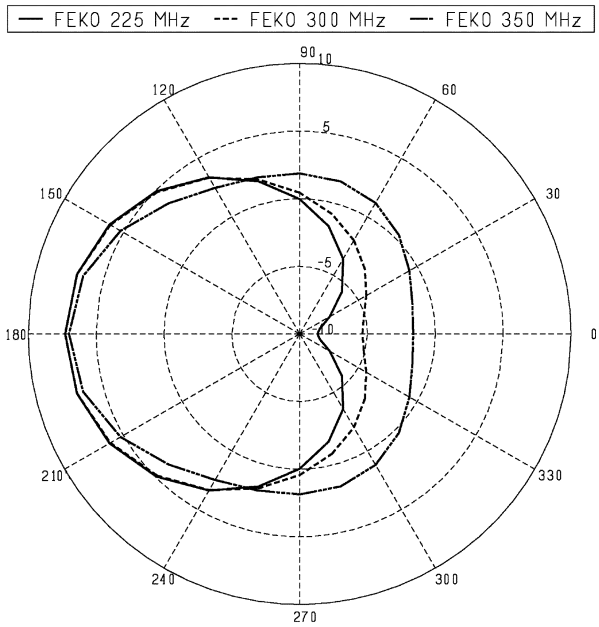

Fig. 6. Radiation pattern (dBi) ($\phi = 0°$ to $360°$, $\theta = 90°$, $\hat{\theta}$ polarized) at the low-band mode.

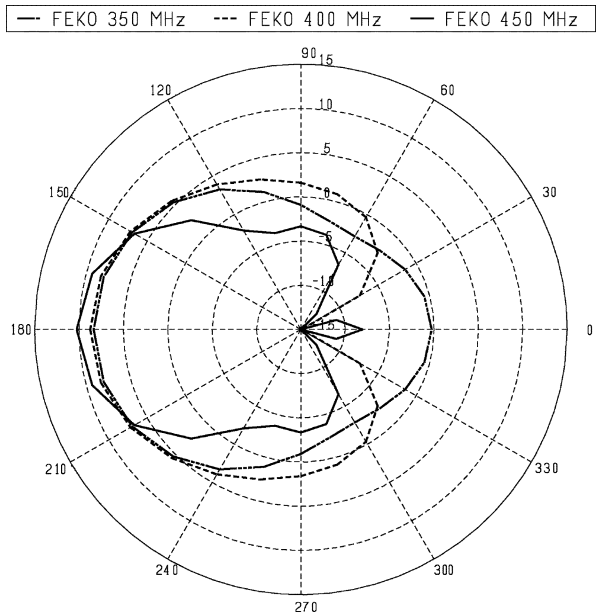

Fig. 7. Radiation pattern (dBi) ($\phi = 0°$ to $360°$, $\theta = 90°$, $\hat{\theta}$ polarized) at the high-band mode.

transition between low and high mode (∼350 MHz) where it is at least 8 dB. Again, HFSS and FEKO predict similar passband and stopband behavior for both low- and high-gain modes. The FBR discrepancies at 250 and 450 MHz between HFSS and FEKO are primarily due to far-field computation of the back radiation of the array. It is understandable that more variation is to be expected for far-field computations at or in the vicinity of the pattern null, since the radiated fields tend to be weak.

The radiation patterns of the array are shown in Figs. 6 and 7. At the low-band mode, at 225 MHz, the pattern is a cardioid shape. As seen in Fig. 6, the null depth gradually degrades and consequently the FBR decreases as the frequency increases. When array is switched to the high band mode, the

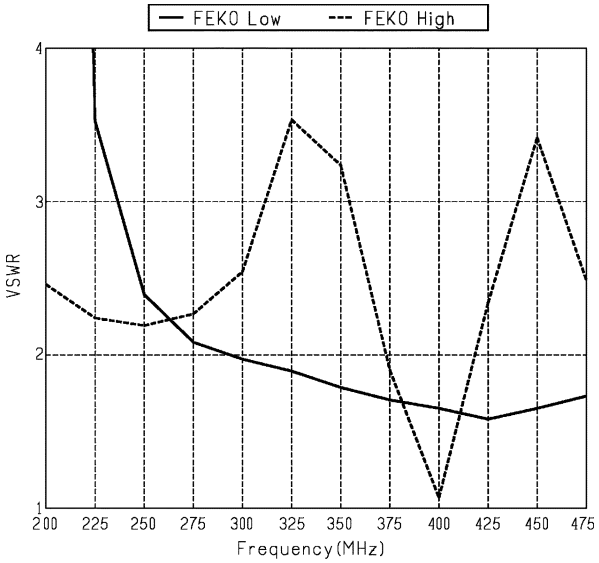

Fig. 8. VSWR versus frequency.

pattern is initially similar to the low band pattern at 350 MHz. However, as the frequency increases, the null depth improves and the cardioid pattern is restored (Fig. 7). Due to the rotational symmetry of the array, the pattern can be rotated around the azimuthal plane at 30° steps by sequential switching of the parasitic loading.

The achieved VSWR in the entire band is 3.5:1 or better as shown in Fig. 8. The characteristic impedance (Z_0) of the array is 150 Ω, as the Z_0 of the biconical driven element at the 35° flare angle in free space is also 150 Ω [8]. While the biconical element easily achieves 2:1 VSWR in the 225–450 MHz band in free space, the presence of the parasitics in the array presents inevitable perturbations to the VSWR. Therefore, the resulting VSWR of the array is expected to be somewhat degraded compared with the biconical element in free space.

IV. Conclusion

A switched parasitic array antenna covering 225–450 MHz band (2:1 bandwidth) has been presented. Simulation results show an antenna gain of 6 to 10 dBi. A VSWR of 3.5:1 or better in the entire band was observed in the simulated results. Due to the rotational symmetry, the main beam can be steered around the azimuthal plane by sequential rotation of the parasitic loading. FEKO MoM simulations were verified using Ansoft HFSS on a few key results. We saw good agreements between HFSS and FEKO. Future work involves manufacturing and measurements of an array prototype.

References

[1] R. F. Harrington, "Reactively controlled directive arrays," *IEEE Trans. Antennas Propag.*, vol. AP-26, no. 3, pp. 390–395, May 1978.

[2] T. Ohira and K. Iigusa, "Electronically steerable parasitic array radiator antenna," *Electron. Commun. Jpn.*, vol. 87, no. 10, pt. 2, pp. 25–45, Jan. 2004.

[3] Y. Nakane, T. Noguchi, and Y. Kuwahara, "Trial model of adaptive antenna equipped with swithced load on parasitic elements," *IEEE Trans. Antennas Propag.*, vol. 53, no. 10, pp. 3398–3402, Oct. 2005.

[4] O. Shibata and T. Furuhi, "Dual-band ESPAR antenna for wireless lan applications," in *Proc. 2005 IEEE Antennas Propag. Symp.*, Jul. 2005, pp. 605–608.

[5] T. Noguchi, T. Yosuke, Y. Nakane, and Y. Kuwahara, "Multi-band adaptive array antenna by means of switched parasitic elements," in *Proc. 2003 IEEE Antennas Propag. Symp.*, Jun. 2003, pp. 916–919.

[6] R. Schlub, D. Thiel, J. Lu, and S. G. O'Keefe, "Dual-band six-element switched parasitic array for smart antenna cellular communications systems," *IEE Electron. Lett.*, vol. 36, no. 16, pp. 1342–1343, Aug. 2000.

[7] J. J. H. Wang, D. J. Triplett, and C. J. Stevens, "Broadband/multiband conformal circular beam-steering array," in *Microwave Symp. Digest 2005 IEEE Microw. Theory Techn. Symp.*, Jun. 2005, pp. 1883–1886.

[8] J. Kraus, *Antennas*. New York: McGraw-Hill, 1988, ch. 8.